Journal of Structural Geology, Vol. 3, No. 4, pp. 393 to 400, 1981.
Printed in Great Britain

0191-8141/81/040393-08 $02.00/0
Pergamon Press Ltd.

Fault movements and stress accumulation before the 1976 Tangshan earthquake in North China

ZHAO GUOGUANG and HUANG PEIYU

Seismotectonic Brigade, State Seismological Bureau, Beijing, China

(*Received* 28 *November* 1980; *accepted in revised form* 28 *May* 1981)

Abstract—This paper analyses geodetic data including the results of short baseline and short levelling surveys across active faults, and of relevellings over a wide area collected at Tangshan and in its vicinity during the several years before the 1976 Tangshan earthquake of magnitude 7.8. Using a theoretical model for slip on a fault plane with an arbitrary dip in a viscoelastic half-space, the parameters of the aseismic fault slip prior to the shock are obtained, and the stress changes caused in the area of Tangshan by such slip are estimated. The results are comparable with the seismic activity and the changes in time and space of the *b*-value in the relation $N = \exp(a - bM)$ observed in the same period. It is demonstrated that during 1968–1975 the Cangdong fault, the main NNE-trending active fault in the southwest of the seismic region, had gradually started aseismic right-lateral strike–slip and that the occurrence of the Tangshan earthquake was related to the stress field produced by the slip. Finally, two sequences of periodic earthquake migration that took place in North China during 1966–1976 are discussed in connection with the Tangshan earthquake.

INTRODUCTION

DURING the period 1966–1976 a series of catastrophic shocks occurred in North China. These events including the greatest one, the Tangshan earthquake of magnitude 7.8 on 28 July 1976, nearly all took place along two seismotectonic zones (Fig. 1). The first is the Tan–Lu zone, named after the well-known Tanchen–Lujiang fracture zone; the second is situated in the North China plain and is simply called 'the Plain Seismic Zone'. It contains some major seismic regions extending from Xingtai to Tangshan. Most of the earthquakes took place on active faults of NNE or NE trend. Their focal mechanisms also appear to be attributable to the build up of stress along the tectonic features.

The seismic activity in this period developed in a rather regular pattern as shown in Fig. 2. Two seismically active stages may be distinguished and two sequences of earthquake migration occurred from the southwest of the North China plain to the northeast in each of the stages. The pattern probably implies that all of the events were under the control of similar seismotectonic processes. Recently, Wang Ren *et al.* (1980) proposed a mathematical simulation to account for the seismic transference. By adjusting the tectonic framework, parameters for the mechanical properties of rocks, coefficients of friction on the faults, and the external stress field, five major earthquakes were simulated. In these studies, however, the possible role of aseismic fault movements was not considered.

Some geodetic data indicate that the present-day tectonic deformation has been concentrated not only around seismic faults but also around some aseismic ones before the main shock. From these data we attempt to assess the role of the aseismic fault movements in the development of the 1976 Tangshan earthquake source.

REGIONAL TECTONIC FEATURES

The Tangshan seismic region is situated on the southern border of the Yanshan Range. The Pre-Sinian crystalline basement is covered unconformably by Sinian and Palaeozoic strata which were folded and faulted with a dominant NNE trend during the Mesozoic. Since Tertiary times the North China plain has subsided while the Yanshan range has been upwarped. There are some border faults extending from Zhuoxian county across Baodi county, Ninghe county in the southwest of Tangshan, to Changli (see Fig. 1). On the northern side of this boundary, Early Tertiary rocks are absent and Late Tertiary and Quaternary rocks are not more than a few hundred metres thick, while Tertiary and Quaternary sediments thicken towards the south.

The most active fault in the area considered is the Cangdong fault (see Fig. 1). It appears to coincide with a well-developed Bouguer gravity anomaly gradient. The fault extends from Wuchen across Cangzhou toward Ninghe; it dips to the southeast, and makes up the eastern boundary of a secondary uplift in the subsidence area. According to data from explosion seismic investigations it seems to be also developed in the vicinity of Tangshan and to extend down to the upper mantle (cf. Chen Yuntai *et al.* 1979, Teng Jiwen *et al.* 1975). The analysis of the stratigraphy indicates that it was a continuously active fault throughout the Cenozoic.

Historical earthquakes on and adjacent to the Cangdong fault (Table 1) took place either in the vicinity of Cangzhou or near Ninghe. Such a distribution of earthquakes probably implies that the characteristics of the fault motion were different for different sections of the fault. We imagine that the northern section of the fault, from Cangzhou to Ninghe, was a 'free section' along which creep took place. The stresses caused by the fault

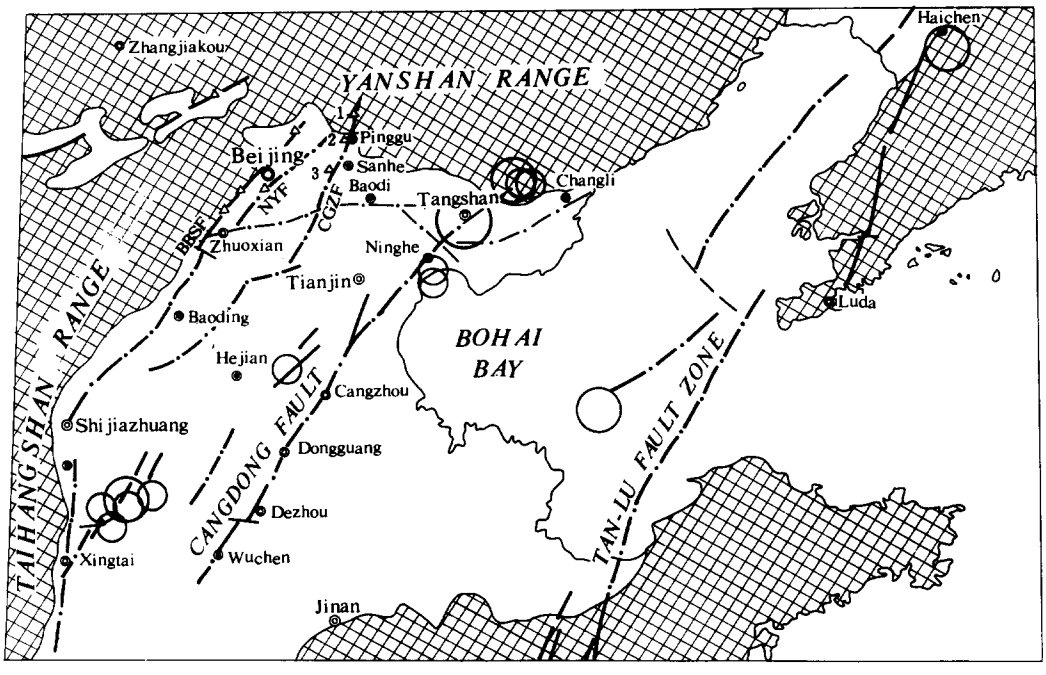

Fig. 1. Seismotectonic sketch map of North China. Epicentres of earthquakes with magnitudes ≧ 6 are illustrated only for the period 1966–1976. CGZF, Chenguozhuang fault; NYF, Nanyuan fault. Triangles represent geodetic stations. Nets represent Cenozoic uplift areas.

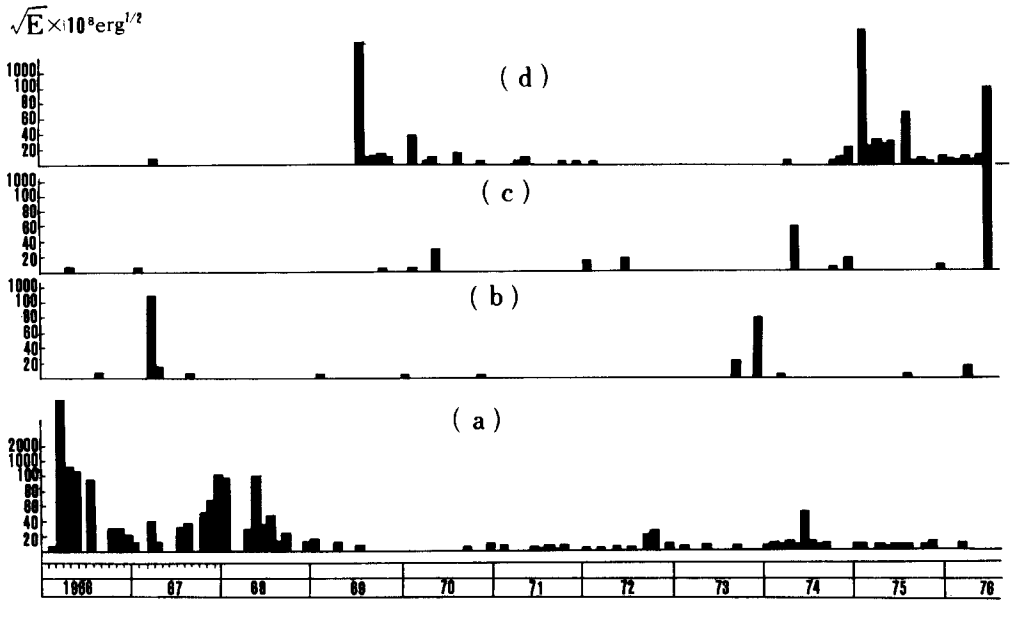

Fig. 2. Two sequences of earthquake migration in North China during 1966–1976, shown by the square-root of monthly-released energy of earthquakes with $M > 3$, for the four seismic regions. (a) The Xingtai region. (b) The Hejian region. (c) The Tangshan region. (d) The Tan-Lu zone.

creep were concentrated near the ends of the fault section and these led to the development of earthquakes. More observational evidence is needed to assess the validity of this idea.

CRUSTAL DEFORMATION IN RELATION TO FAULT MOVEMENTS

Since 1967 we have been monitoring some of the active faults in North China with the aid of short baseline measurements and short levellings across faults. Most of the stations are located in areas where bedrock is exposed. During the period of investigation most of the strong earthquakes occurred in the plain where active faults are buried beneath thick unconsolidated sediments. The only way to evaluate their movements is by determining their deformation effects on the ground surface. During the interval 1956–1976, eleven first-order relevellings in the northern part of North China were accomplished by the

Table 1. Catalogue of historical earthquakes on and adjacent to the Cangdong fault

No.	Date	Location	Lat.	Long.	Intensity	Magnitude
01	14 Aug. 1068	Near Cangzhou	38° 30′	116° 6′	8	(6)
02	18 Jan. 1069	Cangzhou	38° 18′	116° 48′	6	(4¾)
03	April 1625	Cangzhou	38° 18′	116° 48′	6	(5)
04	18 Sept. 1704	Between Cangzhou and Dongguang	38° 0′	116° 30′	7	(5½)
05	6 Aug. 1815	East of Tianjin			6	(5)
06	23 Feb. 1893	Cangzhou	38° 18′	116° 48′	6	(5)
07	19 Jan. 1935	Tangshan	39° 36′	118° 18′	6	(4¾)
08	27 Mar. 1967	Hejian	38° 30′	116° 30′		6.3
09	25 May 1970	Near Ninghe	39° 30′	118° 00′		4.2
10	31 Dec. 1973	Hejian	38° 45′	116° 25′		5.3
11	15 Dec. 1974	Ninghe	39° 20′	117° 35′		4.1
12	1 Dec. 1975	Ninghe	39° 15′	118° 00′		3.7

Geodetic Survey Brigade of the State Seismological Bureau of China (restricted publications). These results provide valuable information on the study of fault movement, and some of them are analysed in the present paper.

Figure 3 shows the vertical crustal deformation in the Tangshan region and its vicinity in the interval 1968–1975, determined from the relevellings. The elevation changes are based on comparisons using the Beijing origin bench-mark as invariant in elevation. It can be seen that the Yanshan range underwent slight uplift while the plain was depressed. In the plain, funnel-shaped subsidence areas formed in the vicinity of some industrial areas such as Tianjin, Beidagang and Tanggu, and these subsidence areas are believed to have been caused by underground-water exploitation. It is noteworthy that there were two pairs of elliptical upheavals and depressions near the ends of the northern free-section of the fault, and that these showed an asymmetric pattern. Their deformation history was different from those in Tianjin and other areas. This can be seen from the profile along the levelling line across Ninghe perpendicular to the Cangdong fault, as shown in Fig. 4. The depression near Ninghe came into being only after 1968 and mainly formed in 1972–1975. Before this time subsidence in Tianjin and other areas showed continuous depression

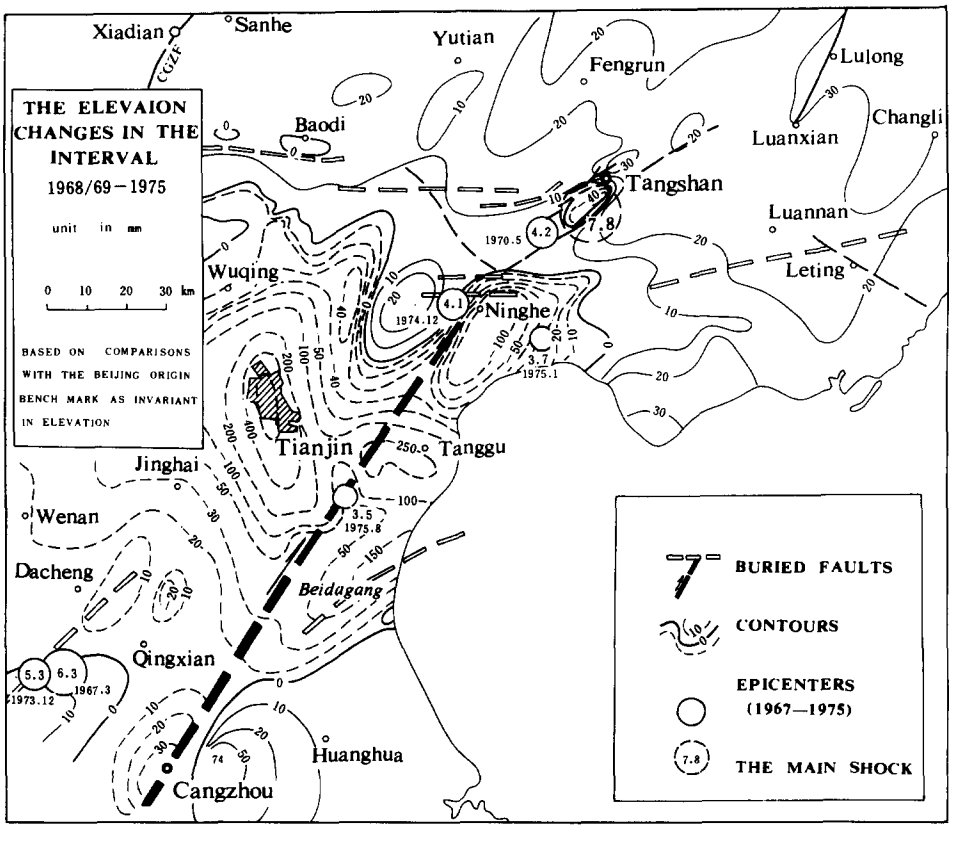

Fig. 3. The vertical deformation in the Tangshan region and its vicinity, measured from the relevellings of the interval 1968/69–1975. The elevation changes are based on comparisons with the Beijing origin bench-mark as invariant in elevation. The contour values are in millimetres.

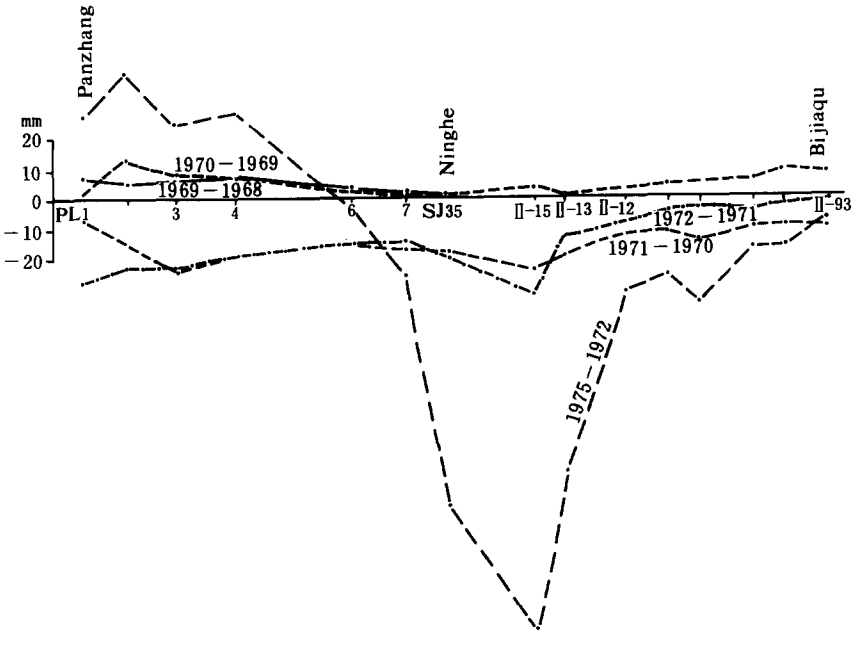

Fig. 4. Profile along the levelling line across Ninghe, perpendicular to the Cangdong fault, showing the deformation history.

over a long period. As to the upheavals, their values are out of all relation to known effects arising from underground-water exploitation.

A reasonable inference can be drawn that the depressions and upheavals developed near Ninghe and Cangzhou were the vertical deformation effects of aseismic slip along the northern section of the Cangdong fault in the interval 1968–1975. According to the dislocation model of a strike–slip fault with a steep dip angle, the vertical deformation on the ground surface near the ends of a fault, is similar to the deformation features that we observed.

In spite of the lack of resurveys along this fault for monitoring the horizontal displacements in the time interval, we have acquired additional information that assures the validity of the proposed inference. First, the features associated with the increment of the Cangdong fault activity were also found on some other faults parallel to it. Figure 5 gives the results from three stations located along the Chenguozhuang fault east of Beijing, and one station located on the Nanyuan fault south of suburban Beijing. The aseismic slip rates on these faults, both horizontal and vertical, increased after 1971 in a way similar to that on the Cangdong fault. It seems likely that the increase in amount of fault slip was also under the control of similar regional tectonic processes. Secondly, if the slip on the Cangdong fault was as large as suggested above, it would cause significant and detectable changes of the stress field in the vicinity of the fault. We should therefore be able to examine them with other methods of investigation. For this purpose, we have to estimate the parameters of the fault slip and the corresponding stress changes with the aid of a suitable theoretical model.

THE MODEL OF THE CANGDONG FAULT SLIP

Rheology of the earth and fault model

Since the late 1950's great progress has been made in theoretical studies of faulting using the elasticity theory of dislocations applied to a seismic fault model, from the inversion of geodetic data, and many successful analyses have been made (e.g. Chinnery 1961, Chen Yuntai *et al.* 1975, 1979). These theories have also been used for problems connected with fault analysis in structural geology (e.g. Chinnery 1966). Strictly speaking, the assumption of the earth as a perfectly elastic body is only suitable for a short time range. According to some authors the mechanical behaviour of the crust and mantle are substantially different over different time intervals. The crust is significantly inelastic over an 'intermediate' interval (say, 4 hours up to 15,000 years), and if the duration is very long, secondary creep (i.e. steady-state creep) will become pronounced (Scheidegger 1963, Jaeger & Cook 1976).

For convenience of making theoretical predictions some rheological models may be used for representing this behaviour. In the case considered in the present paper, it is assumed that the behaviour of a rock medium may be modelled as a generalised Kelvin substance (Price 1964, Jaeger & Cook 1976). Its constitutive equation in one dimension can be written as

$$E_i\left(\eta_k\frac{\partial\varepsilon}{\partial t}+E_k\varepsilon\right)=\eta_k\frac{\partial\sigma}{\partial t}+(E_k+E_i)\sigma \qquad (1)$$

where σ and ε represent stress and strain, respectively; E_i is the instantaneous elastic modulus, E_k and η_k are the

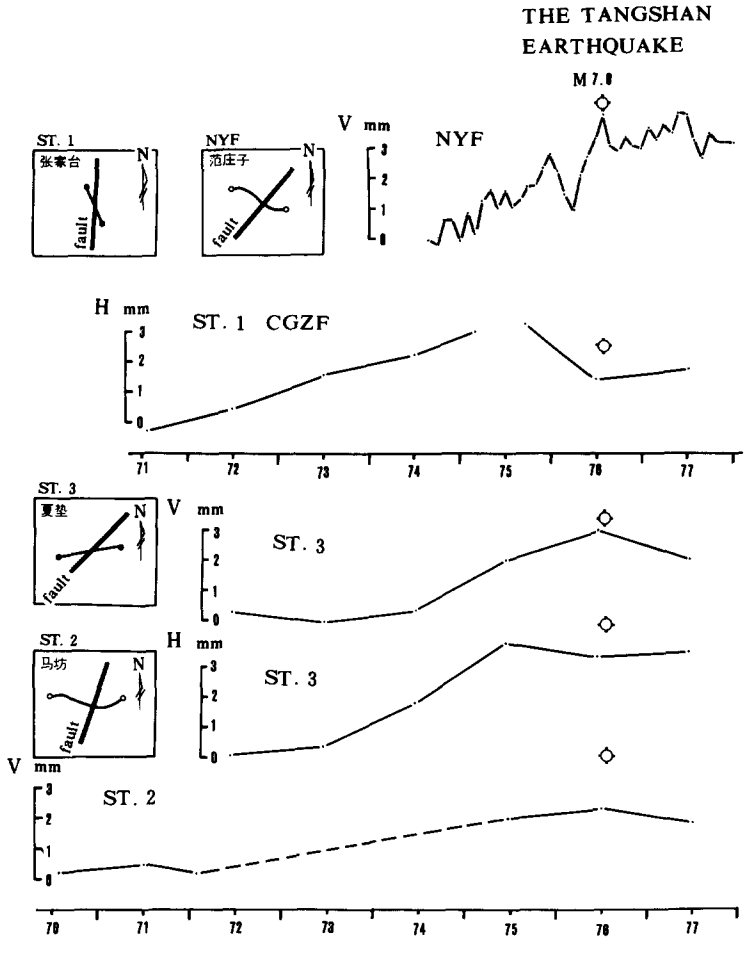

Fig. 5. Relative displacements along the Chenguozhuang fault (CGZF) and the Nanyuan fault (NYF) (see Fig. 1), resulting from short baseline measurements and short relevellings across the faults. H, horizontal; V, vertical displacement. The mountings of measuring lines are also shown in the squares for each station.

Kelvin's constants, and $\partial/\partial t$ denotes differentiation with respect to the time. Clearly, such a substance instantaneously behaves elastically and inelastically when stress is applied during an intermediate time interval.

The fault model is considered as a rectangular plane of $2L$ length, extending from upper boundary, d, down to a lower boundary, D, with an arbitrary dip angle θ, below the free surface of the generalised half-space. The location of the fault with respect to the Cartesian system ($X1$, $X2$, $X3$) is shown in Fig. 6, in which ΔU represents the magnitude of fault slip which is a time-dependent variable and is assumed to be

$$\Delta U(t) = Vt \qquad (2)$$

where V is an average slip rate and t is time.

The analytical expressions of the quasi-static displacements and stress fields caused by such a slipping fault have been developed by the first author (see Zhao Guoguang & Zhang Chao 1981), and will be applied to the Cangdong fault.

The model of the Cangdong fault slip

It can be inferred and measured from Fig. 3 that the slipping section of the Cangdong fault trends N 30°E for a length of 150 km, and that it dips at a steep angle to the SE. Taking the magnitude of slip as $\Delta U = Vt$, $t = 2550$ days (from 1968 to 1975), the average rate V and the other parameters for the slipping section have been deduced

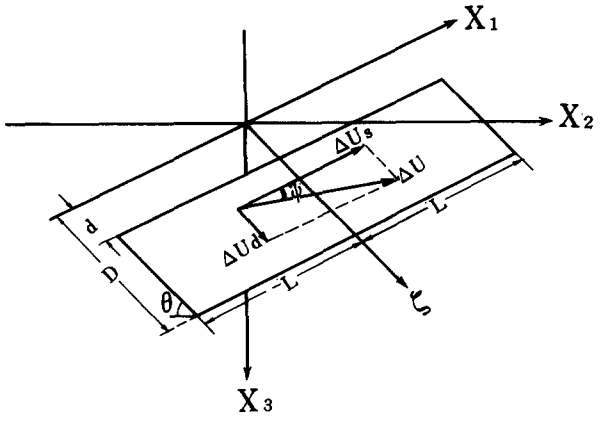

Fig. 6. Geometry of the fault model, showing the location of the fault with respect to the Cartesian system ($X1$, $X2$, $X3$). $2L$, length of the fault; d and D, upper and lower boundary of the fault, measured from the $X1$-axis along the ζ-axis; θ, dip angle; ΔU, the magnitude of the fault slip; ΔUs and ΔUd, strike-slip and dip-slip components respectively.

Table 2. The parameters of the model for Cangdong fault slip derived from the inversion of geodetic data

Strike	Dip direction	Dip angle	Length $2L$ (km)	Upper boundary d (km)	Lower boundary D (km)	Total offset* U (cm)
N30° E	SE	78°	150	1	20	− 61

*Minus stands for the right-lateral strike–slip, while plus indicates left-lateral strike–slip.

from the inversion of the geodetic data. The results appropriate to the measured deformation are listed in Table 2. It shows that, during the interval 1968–1975, the northern free section of the Cangdong fault started an aseismic right-lateral strike–slip, the slip surface had a dip angle of 78°, was 20 km in depth, its upper boundary was about 1 km from the ground surface, and the total offset was −61 cm (minus stands for the right-lateral strike–slip, while plus for the left-lateral strike–slip). This means that the average slip rate increased to the order of several centimetres per year.

Figure 7 gives the comparison between the calculated displacements and the geodetic data. Figure 7(a) is a contour map of the vertical deformation calculated from the model (cf. Fig. 3), and Fig. 7(b) is the profile through Ninghe perpendicular to the fault, in which the solid line represents the theoretical vertical deformation and the datum points are taken from the geodetic surveys near this profile. It will be seen that a good fit was obtained.

Allen & Smith (1966) reported that fresh surface cracking caused by pre-earthquake fault movement had been found preceding the 1966 Parkfield earthquake in California. In our case, however, the horizontal displacements on the ground surface due to the fault slip were not so conspicuous because the deformation effect attenuated with distance from the boundary of the discontinuous slip, which was below the ground surface. We can further examine our deductions by analysing the mechanical effects of the fault slip.

STRESS CHANGES DUE TO THE FAULT SLIP IN THE TANGSHAN REGION

From the model (Table 2), it has been possible to derive the analytical expressions of the stress field for the estimation of the stress changes produced in the Tangshan region by the slip. The relevant results are shown in Fig. 8. The dash–dot contours denote the maximum shear stress on the ground surface, and the hydrostatic stresses are denoted by solid contours for tension and by dashed contours for compression respectively. The contour values are in units of 10^5 dynes cm^{-2}. It can be seen that the maximum shear stress was concentrated around the end of the fault section; while the hydrostatic stress appeared as tension on the right side at the northern end of the fault, and as compression on the left side.

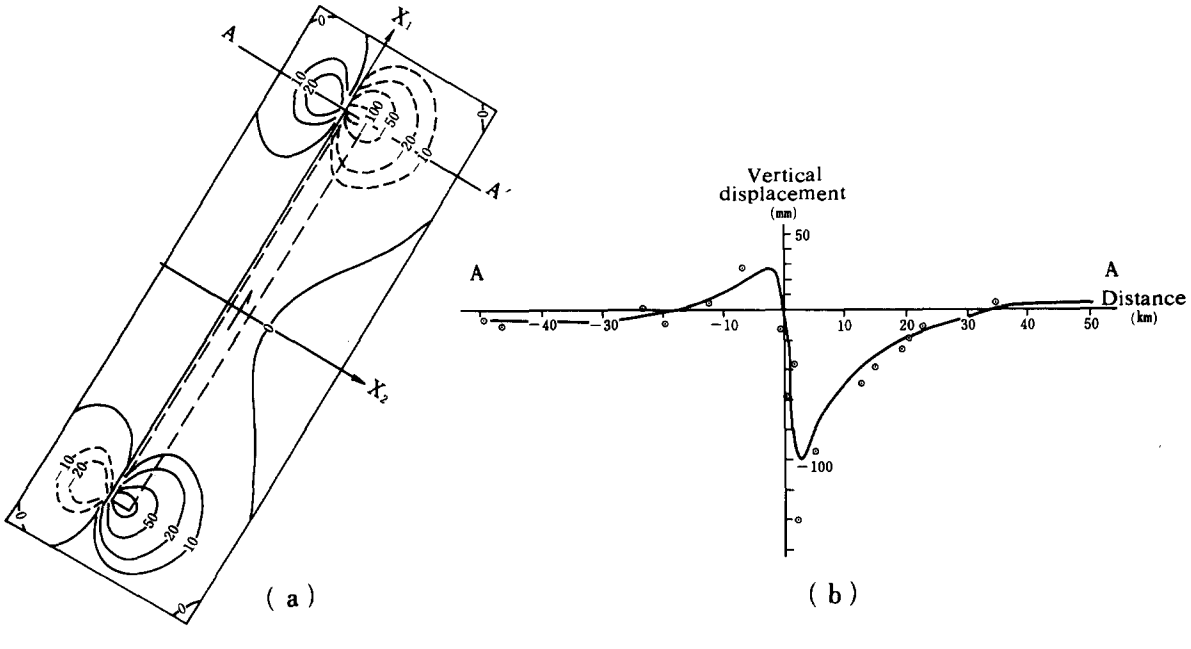

Fig. 7. (a) Contour map of the theoretical vertical deformation calculated from the model for Cangdong fault slip that is comparable with Fig. 3. (b) Profile $A - A'$ showing comparison between the theoretical values (solid curve) and the geodetic datum points.

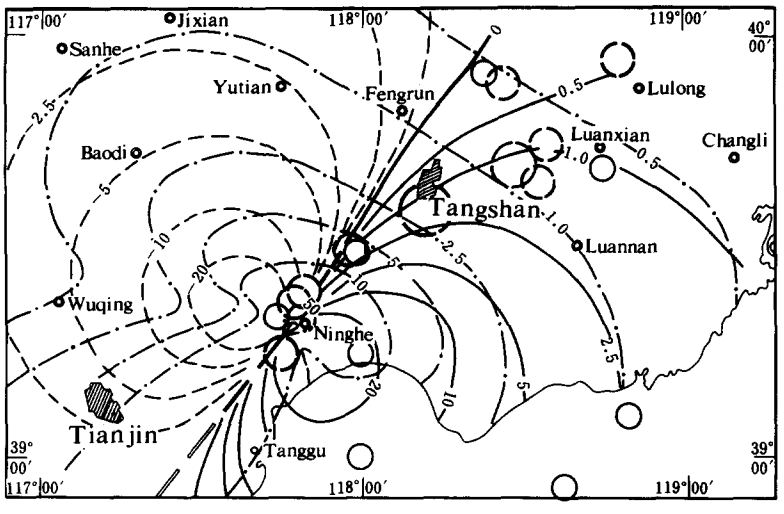

Fig. 8. Stress changes produced in the Tangshan region by the Cangdong fault slip in 1968–1975, calculated from the fault model. Dash–dot contours denote the maximum shear stress, and solid and dashed contours respectively denote the hydrostatic stress in tension and compression. All contour values are in units of 10^5 dynes cm^{-2}. Continuous circles denote epicentres of $M > 3$ earthquakes which occurred from 1970 to 27 July 1976; broken circles denote the Tangshan main shock and its strong aftershocks ($M \geq 6$).

It is of interest to note the relation between the stress pattern and the distribution of the earthquakes that occurred in 1968–1976 (Fig. 8). After 1972, seismicity in the northern part of North China tended to concentrate in the Tangshan region, and some minor shocks occurred in this previously stable region (Qiu-qun 1976, and Table 1). These earthquakes, as well as the great Tangshan earthquake and its strong aftershocks (Fig. 8, broken circles) took place just in the area where the maximum shear stress had increased and the hydrostatic stress appeared to be tensile. It seems a reasonable deduction that the higher shear stress and the increase in hydrostatic tension led to the earthquakes.

The stress pattern can also be compared with the variation of the b-value in the well-known Gutenberg earthquake frequency-magnitude relation

$$N = \exp(a - bM)$$

where M represents earthquake magnitude in the area considered, N is the frequency; and a and b are two coefficients, the latter possibly changing with time and space.

According to some authors (e.g. Mogi 1962, Scholz 1968, Ding Wen-jing 1980), the value of the coefficient b reflects the level of average stress being applied to the region considered, that is, a low b-value implies a high stress level.

Li Quanlin *et al.* (1978, Fig. 9) proposed a time and space scanning of the b-value in North China for studying the development of the Tangshan earthquake. Figure 9(a) shows the spatial distribution of the b-values in the Tangshan region and its surrounding area obtained in 1974–1975. As can be seen, the region of low b-values nearly coincides with the region of concentrated maximum shear stress shown in Fig. 8. Moreover, the time interval of the b-value decline shown in Fig. 9(b) is also

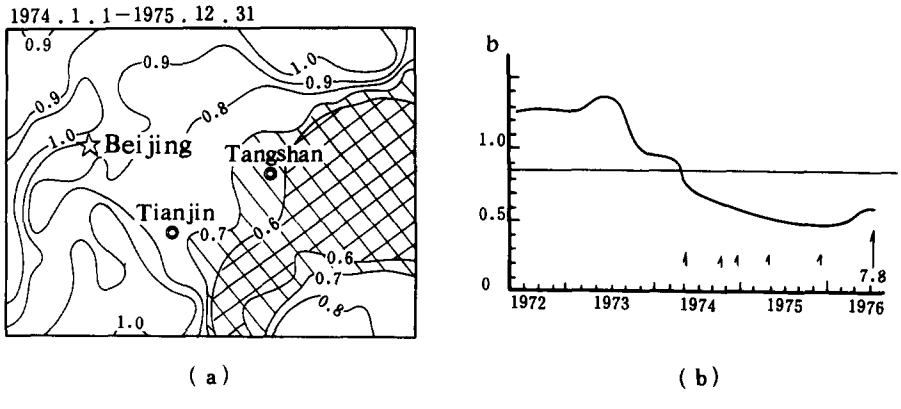

Fig. 9. Time and space scanning of the b-value in the northern part of North China (after Li Quanlin *et al.* 1978, figs. 2 & 5.) (a) Space scanning of the b-value in the Beijing–Tianjin–Tangshin district in 1.1. 1974–31.12. 1975. (b) Time scanning of the b-value in Tangshan and surrounding area.

consistent with the time interval of the stress increase in the same region as the Cangdong fault slip is proposed. Both the seismicity and the variation of the *b*-value in time and space, as indicators of stress change, confirm the fault movement history.

CONCLUSIONS AND DISCUSSION

Geological surveys and mathematical model investigations both lead to the conclusion that the northern section of the Cangdong fault started aseismic slip movement (i.e. creep) before the Tangshan earthquake, and that the earthquake was related to stress changes along the fault as a result of the earlier movement.

Changes in fault activity also occurred at about the same time along some other faults in the Beijing and Tianjin districts, and the various fault movements appear to be genetically linked. We propose that all the aseismic fault movements observed in this early period relate to a regular pattern of early seismotectonic processes controlling regional seismicity.

Acknowledgements — We gratefully acknowledge the Geodetic Survey Brigade, State Seismological Bureau, for the use of their relevelling data, and wish to express our sincere thanks to Professor J. G. Ramsay, Geologisches Institut of E.T.H. Zürich, for comments and helpful suggestions for improving the English of the manuscript. Professors Ma Xingyuan and Wang Ren are thanked for suggestions and a review of an earlier draft in Chinese.

REFERENCES

Allen, C. R. & Smith, S. W. 1966. Parkfield earthquake of 27–29 June, Monterey and San Luis Obispo counties, California. Pre-earthquake and post-earthquake surficial displacements. *Bull. seism. Soc. Am.* **56**, 966–967.

Chen Yuntai, Lin Banghui, Lin Zhongyang & Li Zhiyong 1975. The focal mechanism of the 1966 Xingtai earthquake as inferred from the ground deformation observations. *Acta geophys. sin.* **18**, 164–183. (in Chinese)

Chen Yuntai, Huang Liren, Lin Banghui & Wang Xinghua 1979. A dislocation model of the Tangshan earthquake of 1976 from the inversion of geodetic data. *Acta geophys. sin.* **22**, 201–217. (in Chinese)

Chinnery, M. A. 1961. The deformation of the ground surface faults. *Bull. seism. Soc. Am.* **50**, 355–372.

Chinnery, M. A. 1966. Secondary faulting. *Can. J. Earth Sci.* **3**, 163–174.

Ding Wen-jing 1980. Physical basis of earthquake prediction by the *b*-value. *Acta seism. sin.* **2**, 378–387. (in Chinese)

Jaeger, J. C. & Cook, N. G. W. 1976. *Fundamentals of Rock Mechanics, 2nd Ed.* Chapman & Hall, London.

Li Quanlin, Chen Jinbiao, Yu Lu & Hao Bailin 1978. Time and space scanning of the *b*-value, a method for monitoring the development of catastrophic earthquakes. *Acta geophys. sin.* **21**, 101–125. (in Chinese)

Mogi, K. 1962. Study of the elastic shocks caused by the fracture of heterogeneous materials and its relation to earthquake phenomena. *Bull. Earthq. Res. Inst. Tokyo Univ.* **40**, 125–173.

Price, N. J. 1964. A study of the time strain behaviour of coal-measure rocks. *Int. J. Rock Mech. Min. Sci.* **1**, 277–303.

Qiu-qun 1976. On the background and seismic activity of the $M = 7.8$ Tangshan earthquake, Hebei province of July 1976. *Acta geophys. sin.* **19**, 259–269. (in Chinese)

Scheidegger, A. E. 1963. *Principles of Geodynamics, 2nd Ed.* Springer-Verlag, Berlin.

Scholz, C. H. 1968. The frequency–magnitude relation of microfracturing in rock and its relation to earthquakes. *Bull. seism. Soc. Am.* **58**, 399–415.

Teng Jiwen, Wang Guocheng, Liang Wendou & Xu Shilin 1975. Crustal structure of the central part of the North China Plain and the Xingtai earthquake (II). *Acta geophys. sin.* **18**, 196–207. (in Chinese)

Wang Ren, He Guoqi, Yin Youquan & Cai Yong-en 1980. A mathematical simulation for the pattern of seismic transference in North China. *Acta seism. sin.* **2**, 34–42. (in Chinese)

Zhao Guoguang & Zhang Chao 1981. Quasi-static deformation accompanied by precursory creep and post-seismic fault slip. *Acta seism. sin.* **3**, 217–230.